

M.Eng Project: Automated LBBB Diagnosis Tool, Implemented Using the Discrete Time Wavelet Transform

Joshua Bainbridge (250869629)

Faculty of Electrical and Computer Engineering, Western University

Abstract-In this report an automated electrocardiogram (ECG) detection and annotation algorithm was developed base on the works presented in *Martinez et al.* [1], *Zusterzeel et al.* [2], and *Smisek et al.* [3]. The algorithm was coded in MATLAB and uses the discrete time wavelet transform and multiple layers of segmentation to isolate important components of a raw ECG signal. The results are compared to the Strauss definition of left bundle branch block (LBBB) to produce a diagnosis for a patient.

Key Terms: Electrocardiogram (ECG), ECG Leads, QRS Complex, MATLAB, Discrete Time Wavelet Transform, Delineator, Segmentation, Strauss Definition

1. Introduction

Analysis of electrocardiograms (ECGs) is a very important tool when diagnosing or monitoring the existence and progression of cardiac disease in patients. Computer guided automated detection techniques capable of accurately identifying ECG signal structures can deliver vital information such as heart rate and beat alignments. This information is extremely valuable to medical professionals.

Many algorithms that can automatically delineate a raw ECG signal, isolate locations in the signal and detect the presence of signal artifacts linked to cardiac disease, have been developed with varying levels of success. Within recent years automated ECG algorithms have been developed employing the use of wavelet transforms to identify key areas of interest of an ECG signal.

The following report evaluates an implementation of a wavelet transform based delineator algorithm, coded in MATLAB, used in the automated detection of left bundle branch block (LBBB).

2. Background

Electrocardiogram

An ECG is a medical procedure used to measure the electrical activity of the heart [4]. An ECG is performed by placing ten non-invasive electrodes on a patient. The measurements from the electrodes are analyzed to produce electrocardiographs of the electrical activity of the heart, referred to an ECG [5].

Electrocardiogram leads represent the difference in electrical potential measured in at least two, but often three, electrodes in space [4]. A standard ECG produces twelve leads: six limb leads (I, II, III, aVR, aVL and aVF), as well as six chest leads (V1, V2, V3, V4, V5, V6), as shown in Figure 1, 2.

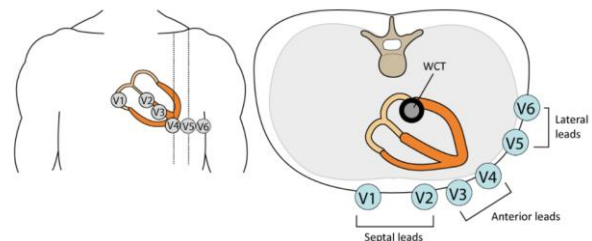


Figure 1. Chest Leads of Standard ECG

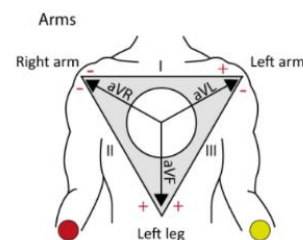


Figure 2. Arm and Leg Leads of Standard ECG

Signal Components of ECG

An ECG wave has three distinct structures: P-wave, QRS complex and T-wave [6]. A P-wave occurs as a result of the depolarization of the left and right atrium. A T-wave occurs as a result of the rapid repolarizations of cells in the heart.

A QRS complex represents the depolarization of the right and left ventricle. However, the vector generated by the depolarization of the right ventricle is much smaller than the vector generated by the left ventricle. Therefore, the QRS is considered a reflection of left ventricular depolarization.

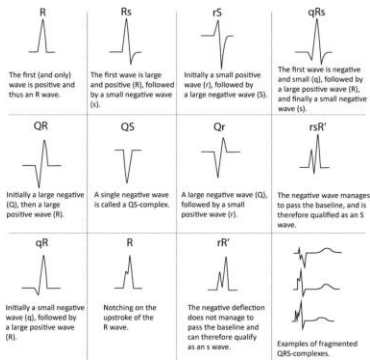


Figure 3. Structures of the QRS Complex [7]

The QRS can have a variety of shapes [8]. This variable QRS morphology presents a unique challenge for automated ECG annotation algorithms. The data used in the testing of the final algorithm was provided by Dr. Antipervitch from the Schulich School of Medicine. The most common QRS structures in the LBBB data set provided by Dr. Antiperovitch, are rS, RS, QRS and QS, Figure 3. Each of these QRS complex shapes are named based on the type and size of wave that is present.

Left Bundle Branch Block

Left bundle branch block (LBBB) occurs when there is a disruption along the bundle branch which blocks or delays the electrical impulse that controls the contraction of the ventricles [5]. The disruption causes a delay between the contraction of the septal and the left ventricle. This results in very inefficient left ventricular contraction [6].

The Strauss definition of LBBB [10]:

QRS \geq 140 ms for men, \geq 130 ms for women, and Q or rS in V1 and V2, and Notching or slurring in \geq 2 V1, V2, V5, V6, aVL

Previous Works

The methodology of the final algorithm in this report closely follows previously successful automated ECG annotation and automated LBBB detection algorithms. The algorithm presented in this report uses an R-wave peak identification and ECG signal delineator methodology based on those published in *Martinez et al.* [1], *Zusterzeel et al.* [2], and *Smisek et al.* [3].

3. Methodology

Description of the Algorithm

The final algorithm presented for this project can automatically evaluate digitized ECG data for the existence of signal artifacts that suggest a patient has LBBB. The algorithm is divided into three stages, each assessing a specific criteria of the Strauss clinical definition of LBBB.

The first stage of the algorithm is R wave peak detection and QRS structure classification. Stage one utilized the discrete time wavelet transform (DTWT) to identify the locations in time of the R-wave peaks. Each R-wave peak found by the DTWT algorithm marks the location of a QRS complex.

Further analysis was conducted on the R-peak locations in stage one on leads V1 and V2. As per the Strauss definition, the structure of the QRS complex in these leads must have either QS or rS shapes.

QRS segmentation is stage two of the algorithm. Multiple segmentation operations were conducted on the ECG signal. Segmentation was performed to determine the start-time and end-time of the QRS complex. Once the start and end times of the QRS are isolated, the duration of the QRS can be calculated. Additionally, the start and end-times from each lead was used to calculate the full duration of the QRS. The result is then compared to the first criteria of the Strauss definition of LBBB.

Notch and slur detection is stage three of the algorithm. Stage three selects segments of the QRS based on the classification denoted in stage one and evaluates changes in the signal's slope to detect the locations of notches or slurs. For QRS complexes classified as rS and QS, notching and slurring can occur along the descending and ascending regions of the S-wave. For QRS complexes classified as QRS and RS,

notching and slurring can occur along the ascending and descending regions of the R-wave. When two or more slurs or notches are detected, the final Strauss criteria has been met and the algorithm will evaluate the patient is likely to have LBBB.

The output of the final algorithm is an overlaid graph of all five analysed leads with all detected notches and slurs denoted and the full duration of the QRS outputted in the console window.

R-wave Peak Detection and QRS Structure Classification

The DTWT is used to identify the locations in time of the R-wave peaks. The structure of each QRS complex found by the DTWT algorithm was then classified.

A) R-wave Peak Detection

Detection of R-wave peaks in the input ECG data was done using the DTWT. The implemented algorithm was derived from the algorithms used in the background papers and online MATLAB signal processing and wavelet toolbox resources [11].

In the final algorithm, R-peaks are detected in a given input signal when the function *find_RPeaks* is called. The function *find_RPeaks*, constructs a 'sym 4' prototype wavelet. The 'sym 4' wavelet was used because it is a wave function that very closely resembles the shape of the QRS complex wave found in an ECG, as shown in Figure 4. This wavelet is the same prototype wavelet used in *Martinez et al.* [1].

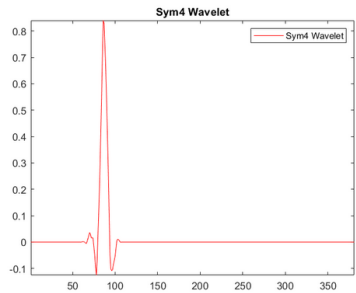


Figure 4. Prototype Wavelet

Due to quantization error and the existence of notches and slurs in the ECG signals, R-wave peak detection could not be directly implemented with the raw ECG input data. It was found that when a R-wave had a severe notch, the *find_RPeaks* function would mark the signal artifact as the peak of the R-wave, as shown in Figure 5.

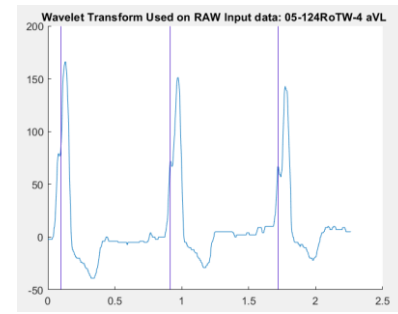


Figure 5. Severe Notching Resulting in Incorrect R-wave Peak Detection

As a result, the input ECG signal first had to undergo signal smoothing preprocessing. This was accomplished by implementing the MATLAB *movmean* function [12]. To eliminate severe notches and slurs the sliding window length was set to 21. A window length of 21 was selected after extensive testing with test data sets. A sliding window of 21 was the minimum value found to consistently remove severe notches and slurs.

After completely removing any possible notches and slurs from the input data the *find_RPeaks* function was called. The function returned R-wave peak times and the raw input signal were then passed into an R-wave peak correction algorithm. The function implemented as *R_Correction* started at the given R-wave peak time and then traversed the raw data to find the corresponding R-wave peak time for the input signal, as shown in Figure 6.

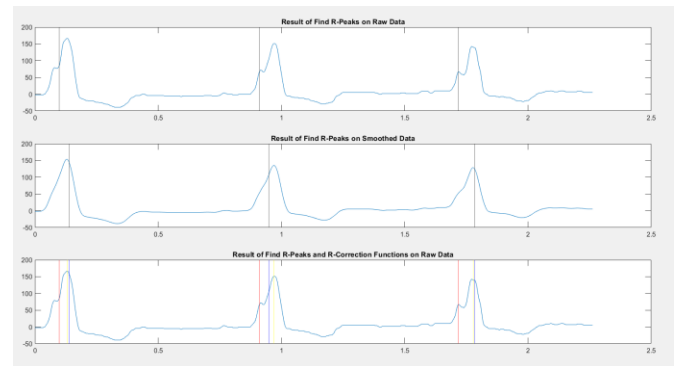


Figure 6. Example of R-wave Peak Correction. Raw data R-peak locations (red), Smoothed data R-peak locations (blue), Corrected R-peak locations (yellow)

B) QRS Complex Classification

Given the time limitations a rudimentary classification system was implemented. For a QRS complex structure to be classified as a rS shape, the ECG signal exhibits an initially

small positive R-wave followed by a larger negative S-wave. Clinically, the S-wave has to have an amplitude seven times greater than the amplitude of the R-wave [13].

Due to time constraints rather than comparing the amplitudes of both the R and S-waves, the classification was done using the R-wave amplitude of the smoothed signal data only. The algorithm found the R-wave peak and then classified an amplitude greater than 50 mV as a RS or QRS wave and amplitudes less than 50 mV were classified as rS.

QRS Segmentation

Multiple segmentations operations were conducted on the ECG signal. Segmentations were performed to determine the start-time of the QRS complex and the end-time of the QRS complex.

A) QRS Complex Start-time

The start-times for each QRS complex in the input data was found individually. The input signal was segmented between two R-wave peaks. The segmentation ranged from the R-wave peak time of the previous QRS complex (QRS_{n-1}) to the R-wave peak of the target QRS complex (QRS_n). In the case $n=1$, QRS_{n-1} was replaced with the signal start-time.

The start-time segmentation was then smoothed, to remove any artifacts that were caused by the quantization of the input signal. The *movmean* function was used with a sliding window of 11. Starting from the peak, the algorithm stepped down the ascending R-wave until a minimum voltage value was reached.

In the cases where the shape of the complex was rS, QS or RS, no negative Q-wave is present, and the location of the minimum value represents the start-time of the QRS complex. In the case the QRS complex is in the QRS formation, the minimum value detected by the start-time function will be at the trough of the Q-wave.

To correct for this, the algorithm evaluates the next five time-steps of every potential start-time point, ($tm_{n-1}, \dots, tm_{n-5}$). The methodology used in this traversing correction is based on early stop techniques used in machine learning [14]. If the voltage difference between each time step is greater than 20% of the potential start-time, the algorithm would continue. The 20% stopping parameter was selected after testing with the test data sets. Future work should conduct more robust testing of this parameter.

In addition to aiding the algorithm in determining an accurate start-time for a QRS structure, the traversing correction was also added so smoothing was not the only method being used to overcome noise in the signal that came as a result of digitization.

B) QRS Complex End-time

In order to determine the end-time of the QRS complex additional considerations were required when compared to the methods used to find the start-time. One of the characteristics of patients with LBBB is a substantially wider QRS complex. One effect this wider QRS can have on the ECG signal is it can cause the S-wave to merge with the T-wave.

In order to accurately evaluate the time corresponding to the end of the QRS complex and the start of the T-wave, a multiple segmentation approach was employed. The first segmentation was conducted on the raw input data. The segment was selected between the R-wave peak time of the target QRS complex (QRS_n) and the QRS start-time of the next QRS complex (QRS_{n+1}). In the case the n was equal to the number of QRS complexes in the input signal, QRS_{n+1} was set to the end-time of the input signal.

The segment was then smoothed using *movmean*, with a sliding window of 11. The *islocalmin* function [15] was then applied to the smooth ECG signal. The local minima produced were compared to returned value. The value returned corresponded to the lowest value of the S-wave.

Once the minimum point of the S-wave was found, the algorithm traversed forward in time to find the peak of the T-wave. The traversing correction method was also employed during this stage of processing. A second segmentation was conducted on the smoothed ECG signal between the S-wave minimum and the T-wave peak.

The instantaneous slope was calculated at each point in the segment by taking the first derivative of the signal, *Equation 1*. The smallest slope in the segment was determined to be the transition point between the leveling off ascending S-wave and the beginning of the ascending T-wave. This transition point was selected as the QRS complex end-time.

$$\dot{x}_t = \frac{x_{t+1} - x_{t-1}}{2\Delta t} \quad \text{Equation 1}$$

Notch and Slur Detection

The final element required for the diagnosis of LBBB is the presence of notches or slurs in the QRS complex. Different

QRS structures have different regions of interest where notching or slurring is likely to occur. The final stage of the algorithm isolated these regions and evaluated them.

A) Notch and Slur Detection: RS and QRS Segmentation

For complexes exhibiting RS or QRS structure, notches and slurs that occur as a result of LBBB present in the positive R-wave of the QRS complex.

Notch and slur detection was done by segmenting the R-wave into two sections: ascending and descending portions of the wave. If the QRS complex was classified as RS, the span of the first segment was from start-time to R-wave peak time. If the QRS complex was classified as QRS, the span of the segment ranged from the Q-wave minimum time to R-wave peak time.

The addition of the Q-wave ascending slope creates a possible source of error. However, the likelihood of error is minimal because of the small duration of the ascending side of the Q-wave.

For both RS and QRS complexes, the second segmentation was required to span from the time of R-wave peak to the end of the R-wave. The same algorithm used to find the end-time of the QRS complex was employed between the time of R-wave peak and the S-wave minimum value. The minimum slope found was set as the transition point between the R and S-wave and was used as the end-time of the R-wave.

B) Notch and Slur Detection: rS Segmentation

For complexes exhibiting rS structure, notches and slurs that occur as a result of LBBB present in the negative S-wave of the QRS complex. Notch and slur detection was done by segmenting the S-wave into two sections. The descending segment contained the portion of the signal from the R-wave peak time to the time corresponding to the S-wave minimum. The span of the second segment started at the time of the S-wave minimum value to the end-time of the QRS complex.

C) Implementation of Notch and Slur Detection

The second derivative was then taken of each segment. The algorithm then used the *localmin* function to detect any rapid changes in the slope of the segment that are caused as a result of notching or slurring.

$$\ddot{x}_t = \frac{x_{t+1} - 2x_t + x_{t-1}}{(\Delta t)^2}$$

Final Results and Graphical Outputs

The final output of the algorithm is a graph that overlays the QRS complexes of each lead. Slurs and notches are denoted on the leads they have been detected in, as shown in Figure 7. The calculated duration of the QRS complex is produced in the MATLAB console.

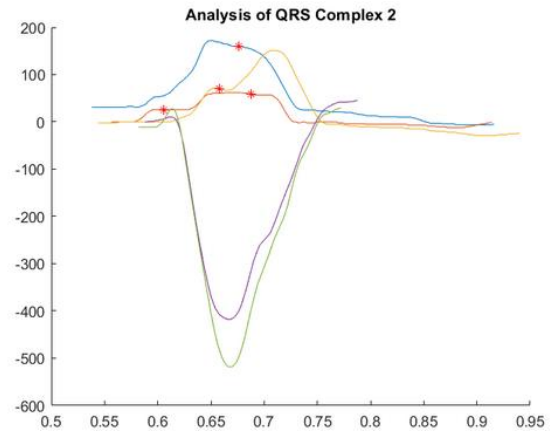


Figure 7. Final Output

4. Algorithm Testing

Testing was conducted on each constituent function of the final algorithm, R-wave peak detection, QRS segmentation and notch and slur detection. Additional testing was done during the development phase in order to determine the optimum values assigned to constant parameters such as the size of the smoothing windows, traversing correction margins and QRS signal classification.

Testing was conducted using the sample data used in Python reference code provided by Dr. Antipetrovitch.

Testing Conducted During Development

Smoothing testing was required to determine the values used for the sliding window parameters. This was done in conjunction with preliminary testing of the *find_RPeaks* function and *R_Correction* function. The effect of different sliding window parameters is shown in Figure 8. When signal smoothing was required to filter out quantization error the final algorithm implemented a sliding window parameter of 11. When signal smoothing was required to remove severe notches and slurs from a QRS complex a sliding window parameter was assigned the value of 21. These values were selected because they minimized distortion of the signal while still achieving the desired outcome, Figure 8.

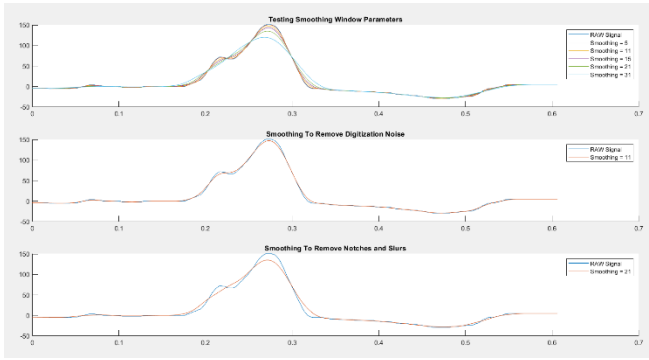


Figure 8. Smoothing Window Parameter Testing

Traversing correction was required to determine the margin that would make the algorithm accurately stop traversing the ECG signal at the QRS start-time. The final margin used in the algorithm was $\pm 20\%$. The value of this parameter was found by testing lead V1, V2, V5, V6 and aVL of one patient.

Description of Available Data for Testing

Four ECG data sets were selected to be used for testing. Each data set was composed of roughly 2.5 seconds of ECG from 12 leads. Leads V1, V2, V5, V6 and aVL from each data set were imported into testing scripts in MATLAB. Across the entire data set 56 QRS complexes were first annotated and classified by hand. The annotations included R-wave peak, start and end-times of each QRS complex.

After classification the number and shape of the QRS complexes found in the data set were as follows: 19 rS, 18 RS, 2 QRS, 11 QS and 6 other structures.

R-wave peak detection

R-wave peak detection was tested on all signals in the testing data set. The *find_RPeaks* function was called, followed by the *R_Correction* function. The test signal was then outputted as a graph with annotations for the predicted peak locations. The results were then manually reviewed, to evaluate the accuracy of the final algorithm.

QRS start and end-times/ Notch and slur detection

QRS start and end-times as well as notch and slur detection were tested on signals with the accurate R-wave peak detection. Due to the fact that the algorithm begins from a detected R-wave peak and delineates out, the algorithm cannot reliably produce results for any QRS without an accurate R-wave peak value. The test signals were then outputted as a graph with the annotations for the start-time,

end-time and predicted notch or slur locations. The results were then manually reviewed, to evaluate the accuracy of the final algorithm.

5. Results

R-wave peak detection

The final results show 37 out of 56 (66%) of R-wave peaks were correctly identified as part of *find_RPeaks* and *R_Correction* functions testing. Full results can be found in the Table 1.

Table 1. R-wave Peak Results

R-Peaks in Leads				<div><div>Correctly Identified</div><div>Incorrectly Identified</div><div>Unidentified</div><div>No Lead Present</div></div>
1	2	3		
005-124RoTW-4				
V1	rS	rS	rS	
V2	rS	rS	rS	
V5	RS	QRS		
V6	RS	RS		
aVL	RS	RS		RS
014-043RoTW-8				
V1	rS	rS	rS	
V2	rS	rS	rS	
V5	QS	QS	QS	
V6	QS	QS	QS	
aVL	RS	RS	RS	
004-021RotE-1				
V1	rsR'	rsR'	rsR'	
V2	rS	RS	RS	
V5	QS	QS	QS	
V6	rS	QS	QS	
aVL	QR	QRS	QR	
014-035RotW-11				
V1	rS	rS	rS	
V2	rS	rS	rS	
V5	RS	RS		
V6	RS	RS		
aVL	RS	RS		RS

QRS complexes with QS structures were the types of QRS structure most often missed by the wavelet-based R-wave peak detection algorithm. If the structures identified as QS are removed from the data set the R-wave peak detection algorithm the accuracy improved to 82% (37 out of 45).

QRS Start and End-Times

Testing was then conducted on QRS complexes with correctly identified R-wave peaks. A total of 24 QRS complexes were used to test the start-time and end-time detection functionality of the algorithm. The final result are shown in Table 2.

Table 2. QRS Start and End-Time Testing Results

R-Peaks in Leads							
	1		2		3		
	Start Time	Stop Time	Start Time	Stop Time	Start Time	Stop Time	
005-124RoTW-4							Correctly Identified Incorrectly Identified Unidentified No Lead Present
V1	0.108	0.316	0.912	1.112	1.726	1.952	
V2	0.104	0.316	0.906	1.096	1.69	1.926	
V5			0.552	0.91			
V6	0.54	0.918	1.314	1.752			
aVL	0.36	0.41	0.808	1.204	1.63	2.056	
014-043RoTW-8							
V1	0.242	0.486	1.104	1.342			
V2	0.048	0.284			1.75	2.006	
V5							
V6							
aVL	1	1.38	1.82	1.938			
004-021RoTW-1							
V1							
V2			0.87	0.992	1.624	1.804	
V5							
V6	0.376	0.832					
aVL	0.476	0.736	1.136	1.806			
014-035RoTW-11							
V1	0.052	0.322	0.86	1.108	1.678	1.944	
V2	0.09	0.312	0.866	1.102	1.69	1.93	
V5			1.504	1.746			
V6	0.576	0.926	N/A	N/A			
aVL			0.836	1.224	1.584	2.104	

The times returned during testing were considered successful if the times found by the algorithm were within 0.01 s of the annotated start and end-times. The algorithm accurately detected 24 start-time and 26 end-times.

Notch and slur detection

Notching or slurring was not present in all of the QRS complexes. A sample of 10 QRS complexes were selected for testing of notch and slur identification. In these cases 80% of the notches and slurs were correctly identified. There were no false positive notches or slurs identified. An example of one unidentified and two correctly identified notches is shown in Figure 9.

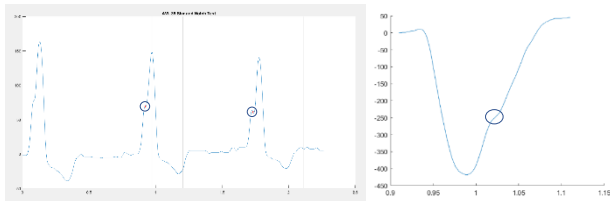


Figure 9. Two Correctly Identified Notches (right) , One missed slur (left)

6. Conclusion

The wavelet transform is a very powerful signal processing tool and has been shown to be very useful in the automated detection and annotation of ECG signals. The use of the wavelet transform was able to accurately detect the R-wave peak of the majority of QRS complexes tested in this project. However, the wavelet transform appears to be highly susceptible to quantization error and large signal artifacts such as severe notching.

Additionally, it is unable to identify QRS complex structures that deviate too much from the prototype wavelet. For example data containing QS waves seem to be undetectable to the wavelet transform. Therefore the wavelet transform, as presented in this project, cannot be the lone method of QRS identification.

Bibliography

- [1] J. P. Martínez, R. Almeida, S. Olmos, A. P. Rocha, and P. Laguna, "A Wavelet-Based ECG Delineator Evaluation on Standard Databases," *IEEE Transactions on Biomedical Engineering*, vol. 51, no. 4, pp. 570–581, Apr. 2004, doi: 10.1109/TBME.2003.821031.
- [2] R. Zusterzeel *et al.*, "The 43rd International Society for Computerized Electrocardiology ECG initiative for the automated detection of strict left bundle branch block," *Journal of Electrocardiology*, vol. 51, no. 6, pp. S25–S30, Nov. 2018, doi: 10.1016/j.jelectrocard.2018.08.001.
- [3] R. Smisek, I. Viscor, P. Jurak, J. Halamek, and F. Plesinger, "Fully automatic detection of strict left bundle branch block," *Journal of Electrocardiology*, vol. 51, no. 6, pp. S31–S34, Nov. 2018, doi: 10.1016/j.jelectrocard.2018.06.013.
- [4] "The ECG leads: electrodes, limb leads, chest (precordial) leads, 12-Lead ECG (EKG) – ECG & ECHO." <https://ecgwaves.com/topic/ekg-ecg-leads-electrodes-systems-limb-chest-precordial/> (accessed Dec. 14, 2021).
- [5] "Electrocardiogram (ECG or EKG) - Mayo Clinic." <https://www.mayoclinic.org/tests-procedures/ekg/about/pac-20384983> (accessed Dec. 14, 2021).
- [6] "ECG interpretation: Characteristics of the normal ECG (P-wave, QRS complex, ST segment, T-wave) – ECG & ECHO." <https://ecgwaves.com/topic/ecg-normal-p->

wave-qrs-complex-st-segment-t-wave-j-point/
(accessed Dec. 14, 2021).

- [7] "QRS Interval • LITFL • ECG Library Basics."
<https://litfl.com/qrs-interval-ecg-library/>
(accessed Dec. 19, 2021).
- [8] "QRS Complexes."
- [9] "Bundle branch block - Symptoms and causes - Mayo Clinic."
<https://www.mayoclinic.org/diseases-conditions/bundle-branch-block/symptoms-causes/syc-20370514> (accessed Dec. 14, 2021).
- [10] P. Antipovitch, "ECG_bioeng," 2021.
- [11] "R Wave Detection in the ECG - MATLAB & Simulink."
<https://www.mathworks.com/help/wavelet/ug/r-wave-detection-in-the-ecg.html> (accessed Dec. 15, 2021).
- [12] "Moving mean - MATLAB movmean."
<https://www.mathworks.com/help/matlab/ref/movmean.html> (accessed Dec. 15, 2021).
- [13] E. A. Ashley and J. Niebauer, "Conquering the ECG," 2004, Accessed: Dec. 16, 2021. [Online]. Available:
<https://www.ncbi.nlm.nih.gov/books/NBK2214/>
- [14] L. Prechelt, "Early Stopping - But When?," pp. 55–69, 1998, doi: 10.1007/3-540-49430-8_3.
- [15] "Find local minima - MATLAB islocalmin."
<https://www.mathworks.com/help/matlab/ref/islocalmin.html> (accessed Dec. 15, 2021).

